

An Infrared Study of the Interactions of CO and CO₂ with Cu/SiO₂

DEAN B. CLARKE, ISAO SUZUKI, AND ALEXIS T. BELL

Chemical Sciences Division, Lawrence Berkeley Laboratory, and Department of Chemical Engineering, University of California, Berkeley, California 94720

Received November 16, 1992; revised February 2, 1993

The adsorption of CO and CO₂ on Cu/SiO₂ have been investigated by infrared spectroscopy. CO adsorbs on Cu with a heat of adsorption of 8.4 kcal/mol, whereas CO₂ weakly adsorbs on both Cu and SiO₂ with a heat of adsorption of 6.9 kcal/mol. As much as 24% of the adsorbed CO₂ is associated with Cu, and the rest with the silica support. On freshly reduced Cu/SiO₂, adsorbed CO exhibits an infrared band 2103 cm⁻¹, whereas CO₂ exhibits a band at 2340 cm⁻¹ when adsorbed on both SiO₂ and Cu surfaces. A band at 2118 cm⁻¹ is also observed during CO₂ exposure. This feature is attributable CO associated with Cu⁺ formed via the dissociation of CO₂ into CO, and O₂. The extent of CO₂ dissociation on Cu is measured to be about 20%. During CO₂ exposure the coverage of adsorbed CO increases rapidly, goes through a maximum, and then decays. This transient is attributable to the competition of CO and CO₂ for Cu sites. The effects on the CO₂ dissociation transient of temperature, pressure, space velocity, catalyst preoxidation, and H₂ addition can be explained with the proposed mechanism. © 1993 Academic Press, Inc.

INTRODUCTION

The interaction of CO and CO₂ with copper surfaces is of considerable importance for understanding the synthesis of methanol from CO and CO₂. Studies by Chinchin and co-workers (1) indicate that CO₂ is the principal source of carbon during methanol synthesis from mixtures containing both CO and CO₂. CO is thought to react in such systems via the water-gas-shift reaction to produce more CO₂. These studies have suggested, as well, that during reaction, CO₂ dissociates to produce O₂, which in turn, oxidizes the surface of Cu particles to produce Cu⁺¹ sites. It has been suggested that the presence of O₂ enhances the adsorption of CO₂ and that the presence of Cu⁺¹ sites enhances the adsorption of CO (1, 2).

The adsorption of CO on supported Cu and unsupported polycrystalline and single crystal Cu surfaces has been studied extensively (3-28). There is general agreement that CO prefers to adsorb on Cu surfaces carbon-end-down in a singly coordinated, on-top position approximately normal to the

surface. The binding of CO on Cu surfaces is weak relative to that on group VIII transition metals, with values ranging from 6-10 kcal/mol for Cu/SiO₂ (10), from 9-16 kcal/mol for Cu powder, from 11-14 kcal/mol for Cu(311) (12), and from 13-17 kcal/mol for Cu(100) (27).

IRAS (3-5), FTIR (6-11), and HREELS (12-15) have been used to study CO adsorption on Cu. For Cu(100), Cu(110), and Cu(311) the CO band is observed at 2085, 2093, and 2102 cm⁻¹, respectively (3). Cu dispersed on oxide supports shows infrared bands for adsorbed CO at relatively high frequencies. Studies conducted with supported Cu have demonstrated the presence of several distinct bands depending on the state of oxidation of the metal (3). For example, Kohler *et al.* (10) report the following band positions for CO adsorbed on Cu/SiO₂: Cu⁰ (2103-2110 cm⁻¹), Cu⁺ (2121-2126 cm⁻¹), and Cu²⁺ (2127-2132 cm⁻¹). Peaks observed at 2175 and 2199 cm⁻¹ are ascribed to CO on isolated Cu⁺ and Cu²⁺ ions, respectively.

The interactions of CO₂ with copper sur-

faces have been investigated much less extensively than those of CO. In an appendix to their paper, Wachs and Madix (29), reported that >99% of the CO₂ adsorbed on a Cu(110) surface dissociated upon adsorption at 180 K. However, subsequent studies by Campbell and co-workers (30) showed no CO₂ adsorption on Cu(110) for exposures up to 350 L at 110 and 250 K. Exposure of the surface to 10³ Torr of CO₂ at 400–600 K led to a slow buildup of adsorbed oxygen due to the process CO₂(g) → CO_s + O_s. More recently, Schneider and Hirschwald (31) reported 100% of the CO₂ adsorbed on Cu(110) at 85 K dissociated upon temperature-programmed desorption. The interactions of CO₂ with a Cu(100) surface have been discussed by Rasmussen *et al.* (32), who found that CO₂ adsorbs molecularly at 79 K with a heat of adsorption of 6.3–7.5 kcal/mol. Exposure of the crystal at 475–500 K led to the progressive accumulation of atomic oxygen on the surface.

Studies of CO₂ adsorption on a polycrystalline foil by Norton and Tapping (33) show that the heat of physisorption of CO₂ is no more than ~ 10 kcal/mol. Evidence for both physisorbed and chemisorbed CO₂ on a Cu foil has been reported by Copperthwaite *et al.* (34). The latter state is proposed to be CO₂⁻_s and is estimated to have a heat of adsorption of 15 kcal/mol. The interactions of CO₂ with Cu powder are described by Hadden *et al.* (35). CO₂ is found to adsorb both molecularly and dissociatively at 293 to 299 K. The room-temperature interaction of CO₂ with Cu/SiO₂ has recently been reported by Millar *et al.* (36). Infrared spectra of the catalyst exposed to 1 atm of CO₂ showed the progressive growth in intensity of a band at 2115 to 2126 cm⁻¹ attributed to CO adsorbed on Cu⁻¹ sites. Based on this evidence and the observation of CO in TPD spectra following exposure of the catalyst to CO₂, it was concluded that CO₂ adsorbs dissociatively at 298 K.

This paper reports the results of an investigation aimed at understanding the interaction of CO₂ with Cu/SiO₂. To this end, *in*

situ infrared spectroscopy was used to observe the species present on the catalyst surface as a function of time and catalyst pretreatment. The heat of CO₂ adsorption and the extinction coefficient for adsorbed CO₂ were obtained as well. An investigation of CO adsorption on Cu/SiO₂ was also carried out to determine the extinction coefficient for adsorbed CO, and the heat of CO adsorption on the catalyst surface.

EXPERIMENTAL

The copper-on-silica catalyst was prepared by ion exchange of fumed silica (Cabosil M-5, 200 m²/g) following the procedure described by Kohler *et al.* (37). The Cu weight loading was measured to be 7.04% by X-ray fluorescence analysis. The dispersion of Cu was determined to be 0.38 from the saturation uptake of CO, assuming a stoichiometry of 0.18 CO molecules adsorbed per surface Cu site (38). This corresponds to a Cu surface area per gram of catalyst of 18.2 m²/g.

For *in situ* infrared experiments, 50 mg of the catalyst was finely ground and pressed into a 2-cm-diameter wafer by applying 7000 psi for 30 s. The catalyst disk was then placed in a low dead volume infrared cell (39). The optical path length between the CaF₂ windows in this cell is 2.4 mm, and the dead volume in the assembled cell is 0.4 cm³. The temperature of the cell was maintained to within 1 K of a preset value by a temperature controller connected to a thermocouple located inside the infrared cell.

Gases were supplied to the infrared cell through Tylan mass flow controllers. The following gases were used: Matheson UHP Ar, H₂, O₂, CO, and 10% N₂O in Ar and Coleman instrument-purity CO₂. A series of traps was used for purification of the gases. Ar was passed through an oxysorb (CrO₃) trap to remove O₂ and then a molecular sieve (Davison 3A, grade 564) trap to remove water. CO was passed through a bed of glass beads maintained at 573 K to remove iron carbonyls and then through an

ascarite trap for CO₂ removal and a molecular sieve trap for water removal. Hydrogen was passed through a Deoxo unit (Engelhard) which removes O₂ impurities by forming H₂O, and then the water was removed by a molecular sieve trap. CO₂ was passed through a hopcalite (80% MnO₂ + 20% CuO) trap to remove CO and a molecular sieve trap to remove H₂O. Reduction of the catalyst was carried out in a flow of H₂ at 1 atm at 513 K for 3 h or more (usually overnight). Partial oxidation of the Cu was achieved by exposing a reduced catalyst to 76 Torr of N₂O at 363 K for 1.5 h. For more severe oxidation, the catalyst was heated in 1 atm of O₂ at 363 K for 1.5 h. These conditions were chosen to prevent bulk oxidation of the Cu which can occur at temperatures greater than 378 K (40).

Infrared spectra were recorded with a Bio-Rad Model FTS-15/80 Fourier transform infrared spectrometer linked to a Model 3200 computer for data acquisition and processing. Between 16 and 256 scans were collected at a resolution of 0.5 to 4 cm⁻¹. Typically, 64 scans per spectrum were taken at 4 cm⁻¹.

Adsorption isotherms of CO and CO₂ on Cu/SiO₂ were measured in a standard glass adsorption system. A 0.5-g sample of Cu/SiO₂ was reduced in flowing H₂ at 513 K overnight. The sample was then evacuated to below 10⁻⁶ Torr, cooled to room temperature, and exposed to progressively higher pressures of the adsorbing gas. The amount of gas adsorbed by the catalyst was calculated from the initial and final equilibrium pressures and the volume of the dosing portion of the glass system.

RESULTS AND DISCUSSION

1. CO Adsorption

Isotherms of the total amount of CO adsorbed on Cu/SiO₂ and the amount adsorbed reversibly are given in Fig. 1. Since only a negligible amount of CO adsorbs on a sample of pure silica, under the conditions indicated, all of the adsorbed CO reported in

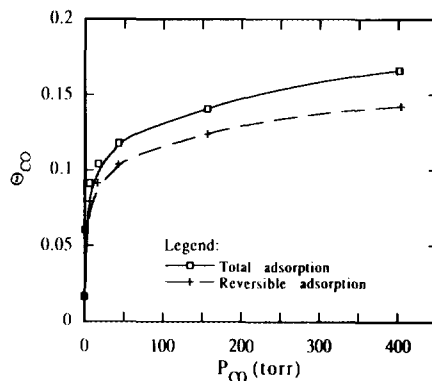


FIG. 1. Chemisorption isotherm for CO on reduced Cu/SiO₂ taken at 303 K. The isotherm for reversible plus irreversible adsorption was measured by exposing a freshly reduced catalyst to CO. The isotherm for reversible adsorption was then measured by evacuating the sample to <10⁻³ Torr for 85 min and then re-exposing it to CO.

Fig. 1 is associated with the Cu particles dispersed on the support. It is immediately apparent from Fig. 1 that the majority of the CO is bound reversibly and only a small fraction is held irreversibly. Taking the saturation coverage of CO at 302 K to be 0.18 ML (38), it is concluded that the Cu surface is nearly saturated at 400 torr, since $\Theta_{CO} = 0.17$.

Figure 2 shows spectra of adsorbed CO taken after 10 min of exposure of the catalyst to 60 Torr CO at 303 K. In each case, a spectrum of a silica disk recorded in the presence of CO has been subtracted from that taken with the Cu/SiO₂ sample, to eliminate spectral features associated with silica and gas-phase CO. Spectrum (a) is for freshly reduced Cu/SiO₂, whereas spectra (b) and (c) are recorded for CO adsorbed on a partially oxidized sample. For the reduced catalyst, a single, asymmetric band is observed centered at 2103 cm⁻¹. The position of the band maximum is characteristic of linearly adsorbed CO on Cu⁰. Adsorption of CO on the sample oxidized in O₂, spectrum (c), results in a shift of the band position to 2122 cm⁻¹. This feature can be ascribed to CO associated with Cu⁺ sites (10). CO ad-

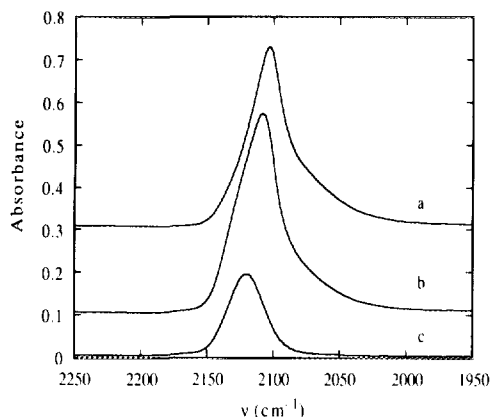


FIG. 2. Infrared spectra of CO adsorbed on Cu taken at 303 K after 10 min of exposure to 60 Torr CO. All spectra were recorded with a resolution of 4 cm^{-1} following which the spectra of gas-phase CO and SiO_2 were subtracted. The catalyst was pretreated with: (a) 760 Torr H_2 for 6 h at 513 K; (b) 76 Torr N_2O for 1.5 h at 363 K; and (c) 760 Torr O_2 for 5.3 h at 363 K.

sorption following oxidation of the sample in N_2O produced spectrum (b). The position of the CO band and its shape in this case are intermediate between those for spectra (a) and (b), suggesting that N_2O preoxidation results in a surface containing both Cu^0 and Cu^+ sites.

Spectrum (a) in Fig. 2 can be deconvoluted into three separate bands centered at 2120, 2103, and 2078 cm^{-1} , corresponding to linearly adsorbed CO on Cu^+ , high-index planes [e.g., $\text{Cu}(211)$, $\text{Cu}(311)$, and (755)] of metallic Cu, and low-index planes [e.g., $\text{Cu}(100)$ and $\text{Cu}(111)$] of metallic Cu, respectively (3). Using the extinction coefficients for CO reported by Kohler *et al.* (10), it is concluded that 11% of the adsorbed CO is associated with Cu^+ sites. In a study of the state of Cu on Cu/SiO_2 , Kohler *et al.* (41) concluded that even after reduction approximately 10% of the total Cu remained as Cu^+ . These sites were attributed to isolated Cu^+ cations attached to two adjacent silanol groups. We believe that at least a part of the Cu^+ tagged by adsorbed CO on the reduced Cu/SiO_2 catalysts studied here might be due to isolated Cu^+ sites. However, in contrast

to Kohler *et al.* (10), we conclude that the frequency of adsorbed CO associated with Cu^+ present as isolated cations on the support and as cationic centers on the surface of Cu particles is the same. This conclusion is supported by the absence of a band at 2170 cm^{-1} , which Kohler *et al.* (10) attribute to CO adsorbed on isolated Cu^+ sites, from the spectrum of adsorbed CO following the subtraction of the spectrum for gas-phase CO. While a weak band in the vicinity of $2166\text{--}2173\text{ cm}^{-1}$ was observed in the spectra recorded in the presence of the gas phase, this feature disappeared upon subtraction of the gas phase spectrum.

Figures 3 and 4 show plots of the position and integrated intensity of the CO band on reduced Cu/SiO_2 as a function of CO coverage at 303 K. The CO coverage was varied by increasing the CO partial pressure from 0.03–200 Torr. As seen in Fig. 3, the position of the CO band shifts from 2110 cm^{-1} to 2102 cm^{-1} as the CO coverage increases. This trend is probably due to preferential adsorption of CO on high index planes of Cu at low CO pressures and to a progressive increase in the fraction of CO adsorbed on low index planes as the CO pressure increases (3). It should be noted that the observed trend in CO frequency with increasing CO coverage is the reverse of that seen

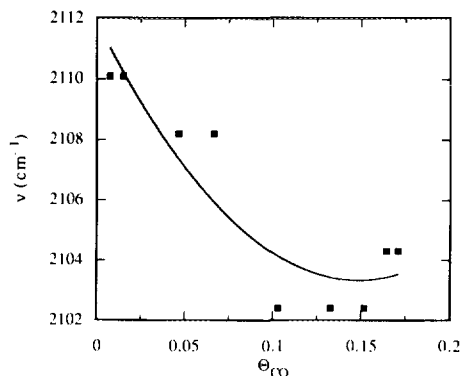


FIG. 3. Dependence of the vibrational frequency of adsorbed CO on the coverage of CO at 303 K. The indicated coverages correspond to pressures between 0.027 and 33 Torr.

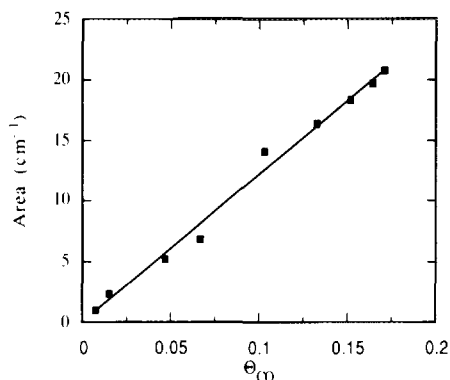


FIG. 4. Integrated absorbance area of the band for CO adsorbed on Cu⁰ versus the fractional coverage of the Cu surface at 303 K. Exposures were at CO partial pressures ranging from 0.027 to 155 Torr.

for transition metals. In that case the frequency of CO vibration rises with increasing coverage, due to a decrease in the extent of *d*-electron backdonation into the π* antibonding orbital of CO.

A linear increase in the integrated absorbance of the CO band with CO coverage is seen in Fig. 4. The extinction coefficient determined from the slope of this line is $3.2 \times 10^{-17} \text{ cm}^{-1} \cdot \text{cm}^2 \text{ molecule}^{-1}$. This value is comparable to that reported for CO adsorbed on Pd/SiO₂, $6.05 \times 10^{-17} \text{ cm}^{-1} \cdot \text{cm}^2 \text{ molecule}^{-1}$ (42), and Ru/SiO₂, $7.47 \times 10^{-17} \text{ cm}^{-1} \cdot \text{cm}^2 \text{ molecule}^{-1}$ (43). An extinction coefficient based on absorbance peak height was also determined. This value is $7.0 \times 10^{-19} \text{ cm}^2/\text{molecule}$, in very close agreement with the value of $6.5 \times 10^{-19} \text{ cm}^2/\text{molecule}$ reported recently by Kohler *et al.* (10).

A plot of the integrated absorbance versus inverse temperature is illustrated in Fig. 5. For this experiment, the pressure was kept at 0.38 torr, to assure a linear relationship between the coverage and the equilibrium constant for adsorption. The coverage of the Cu surface varied from 0.02 to 0.04. Under such circumstances, the heat of CO adsorption can be determined from the slope of Fig. 5. The value obtained in this fashion is 8.4 kcal/mol. This value lies well within the

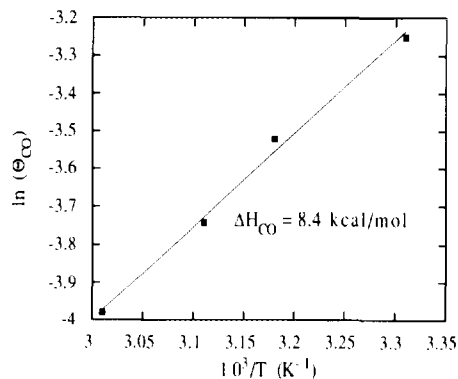


FIG. 5. Clausius-Clapeyron plot for CO adsorbed on reduced Cu/SiO₂ taken with a CO pressure of 0.038 torr. The temperature varied from 303 to 333 K; θ_{CO} is the fractional coverage of Cu by CO.

range of values reported previously for Cu/SiO₂ catalysts (9, 10), 6–10 kcal/mol.

2. CO₂ Adsorption

The adsorption isotherm for CO₂ on Cu/SiO₂ at 299 K is shown in Fig. 6. Evacuation of the sample following adsorption resulted in complete removal of the adsorbate; hence, all of the CO₂ is reversibly adsorbed. The absence of any evidence of CO₂ saturation also indicates that CO₂ is weakly adsorbed.

Infrared spectra of Cu/SiO₂ exposed to

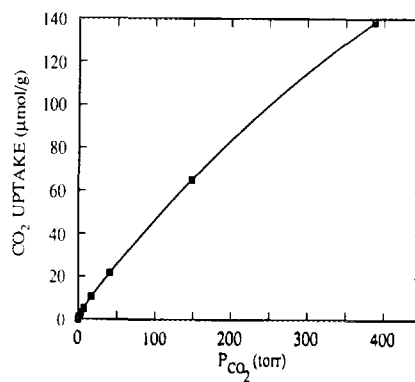


FIG. 6. Adsorption isotherm for CO₂ adsorption on reduced Cu/SiO₂ taken at 303 K.

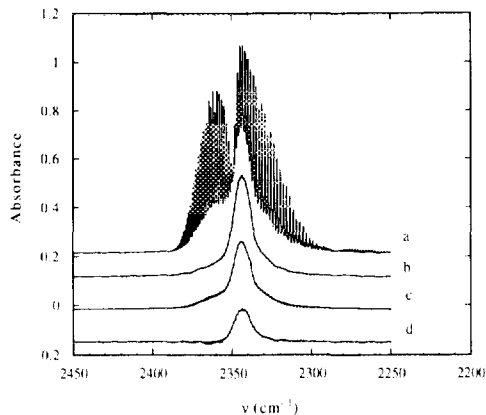
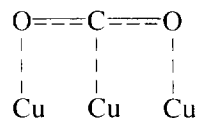


FIG. 7. Infrared spectra of CO_2 adsorbed on reduced Cu/SiO_2 at 303 K and 60 Torr. All spectra were recorded with a resolution of 0.5 cm^{-1} . (a) Total CO_2 spectrum of CO_2 adsorbed on Cu/SiO_2 following the subtraction of a spectrum of Cu/SiO_2 . (b) Surface CO_2 spectrum (a) following subtraction of the gas-phase spectrum of CO_2 . (c) CO_2 on SiO_2 : spectrum of CO_2 adsorbed on a silica wafer following subtraction of the spectrum of SiO_2 and gas-phase CO_2 . The weight of the SiO_2 wafer was the same as the weight of SiO_2 present in the Cu/SiO_2 catalyst for spectrum (a). (d) CO_2 on Cu : spectrum (b) following the subtraction of spectrum (c).

60 torr of CO_2 at 303 K are shown in Fig. 7. Spectrum (a) represents the difference between the spectrum of Cu/SiO_2 taken in the presence of CO_2 and the spectrum of Cu/SiO_2 in argon. Roto-vibrational bands due to gaseous CO_2 are visible superimposed on top of the spectrum of adsorbed CO_2 . Subtraction of the gas-phase spectrum from spectrum (a) results in spectrum (b), which exhibits a single feature centered at 2344 cm^{-1} due to adsorbed CO_2 . Spectrum (c) is for CO_2 adsorbed on SiO_2 and spectrum (d) is the difference between spectra (b) and (c), and, hence, is the spectrum of CO_2 adsorbed only on Cu . The bands seen in spectra (c) and (d) are both centered at 2344 cm^{-1} . If it is assumed that the extinction coefficients for CO_2 adsorbed on SiO_2 and Cu are identical, it can be shown from the integrated peak areas of spectra (c) and (d) that 24% of the CO_2 adsorbed on Cu/SiO_2 resides on Cu .

The stronger interaction of CO_2 with Cu rather than SiO_2 is also supported by purge experiments. Purging in argon results in the immediate desorption of CO_2 from SiO_2 , whereas 12% of the CO_2 adsorbed on Cu/SiO_2 is retained after 1 min of purge. Desorption of the more weakly bound CO_2 adsorbed on Cu shifts the position of the CO_2 band from 2344 to 2340 cm^{-1} . Preoxidation of the catalyst surface with either N_2O or O_2 had no effect on either the position or intensity of the CO_2 band observed after purging of gas-phase CO_2 from the cell. Thus, in contrast to CO , the interactions of CO_2 with reduced and oxidized Cu surfaces seem to be the same.

The position of the band for CO_2 adsorbed on Cu , $2340\text{--}2344 \text{ cm}^{-1}$, is similar to that reported by Force and Bell (44) for CO_2 adsorbed on silica-supported Ag (2350 cm^{-1}). Consistent with their interpretation, we propose that CO_2 interacts weakly with the metal surface as shown below:



An estimate of the extinction coefficient for CO_2 adsorbed on Cu/SiO_2 was determined from measurements of the integrated peak intensity and the amount of CO_2 adsorbed. The resulting value is $2.2 \times 10^{-17} \text{ cm}^2/\text{molecule}$. In making this estimate, it is assumed that the extinction coefficients for CO_2 adsorbed on Cu and SiO_2 are equivalent.

The heat of CO_2 adsorption was estimated from measurements of the integrated intensity of the CO_2 band as a function of temperature. For these experiments, the CO_2 pressure was kept at 150 Torr, the temperature was varied between 303 and 513 K, and the CO_2 coverage of Cu varied from 0.049 to 7.8×10^{-4} . The resulting data are shown in Fig. 8. The heat of CO_2 adsorption determined from the slope of this plot is 6.9 kcal/mol . This value agrees well with that measured for CO_2 adsorption on $\text{Cu}(100)$ (35), $6.3\text{--}7.5 \text{ kcal/mol}$.

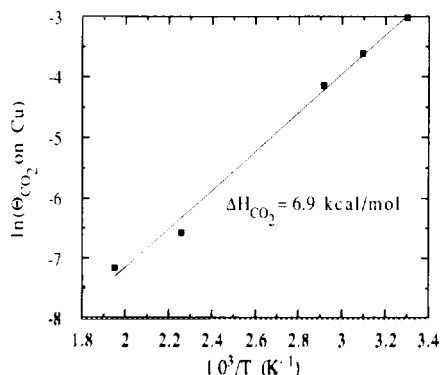


FIG. 8. Clausius-Clapeyron plot for CO₂ adsorbed on reduced Cu/SiO₂ recorded for a pressure of 150 Torr. The temperature varied from 303 to 513 K. θ_{CO_2} is the fractional coverage of CO₂ on Cu.

Figure 9 shows that when the region between 2200 and 2000 cm^{-1} is included in the spectrum of adsorbed CO₂, a band is observed at 2118 cm^{-1} , in addition to that at 2343 cm^{-1} . The band at 2118 cm^{-1} appears only if Cu is present on SiO₂ and is characteristic of CO adsorbed on partially oxidized Cu. The appearance of this feature is attributed to the dissociation of CO₂, to produce CO, and O₂.

The time dependences of the infrared

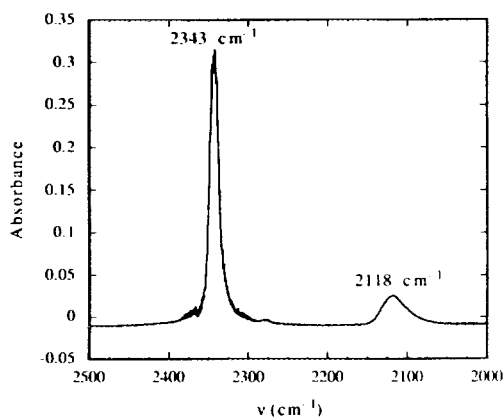


FIG. 9. Infrared spectrum of reduced Cu/SiO₂ exposed to 150 Torr of CO₂ for 10 min at 303 K (resolution = 0.5 cm^{-1}). The spectra of gas-phase CO₂ and SiO₂ have been subtracted.

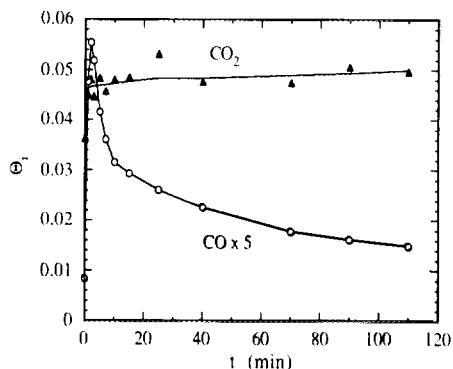


FIG. 10. Time-dependent coverage of Cu by CO and CO₂ during exposure of reduced Cu/SiO₂ to 134 Torr CO₂ at 303 K.

peaks for adsorbed CO₂ and CO are shown in Fig. 10. After exposure to CO₂, the coverages of both CO₂ and CO increase rapidly. The CO₂ coverage then plateaus while the CO coverage goes through a sharp maximum and then decreases. When the infrared cell is flushed with He, the intensities of both peaks fall rapidly, though the CO₂ band is more persistent than the CO band.

The effect of CO₂ flow rate on the dynamics of the CO band observed at 2118 cm^{-1} is presented in Fig. 11. Following the initial transient in CO coverage, the flow rate is rapidly reduced. Each time the flow rate is reduced, the CO coverage increases sud-

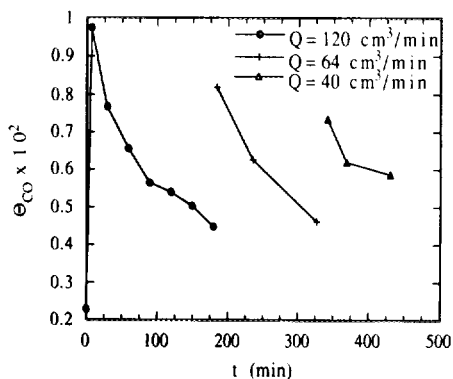


FIG. 11. Effect of flow rate of a CO₂-containing stream ($P_{\text{CO}_2} = 60$ Torr) on the coverage of CO formed via CO₂ dissociation at 303 K.

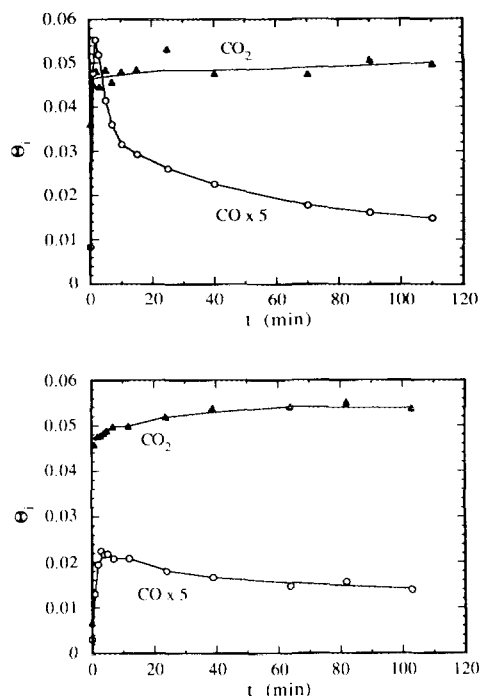


FIG. 12. Time-dependent coverages of Cu by CO and CO₂ during exposure of reduced Cu/SiO₂ at 303 K to (top) $P_{\text{CO}_2} = 134$ Torr and (bottom) $P_{\text{CO}_2} = 59$ Torr.

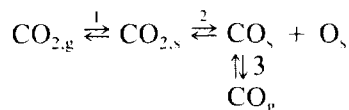
denly and then decays. The steady state coverage of CO₂ on Cu is 0.02 during the first phase of the experiment and is unaffected by subsequent changes in CO₂ flow rate.

Figure 12 demonstrates the sensitivity of the dynamics of CO₂ and CO coverage to the partial pressure of CO₂. With increasing CO₂ partial pressure, the approach of the CO₂ coverage to steady state occurs more rapidly but not the steady-state coverage by CO_{2,s}. Reducing the CO₂ partial pressure causes a reduction in the maximum CO coverage but does not affect the steady-state coverage.

The effects of temperature on the dynamics of CO coverage are illustrated in Fig. 13. As temperature increases, the maximum CO coverage decreases. Increasing the temperature from 343 to 453 K results in a significant decrease in the maximum of the CO_s transient.

The observation of adsorbed CO upon

room-temperature adsorption of CO₂ on Cu/SiO₂ has also been reported recently by Millar *et al.* (36). The process by which CO is formed and the dynamics for the appearance of CO seen in Figs. 10–13 can be explained by the following reaction sequence:



CO₂ rapidly adsorbs from the gas phase and then dissociates to form CO_s and O_s. The dissociation step is slow enough that the adsorbed CO does not build up instantaneously. Both CO and CO₂ compete for sites on the copper surface, and with time the CO₂ displaces CO which desorbs from the surface. Figure 13 shows that during the 2-h period when the CO has yielded about 0.6% of the copper surface, the amount of adsorbed CO₂ has increased by about the same amount. The desorption and readsorption of CO are presumed to be at equilibrium, since the surface coverage of CO responds instantaneously to changes in the flow rate of CO₂ (see Fig. 11).

While the proposed interpretation seems at odds with the fact that more than 95% of the surface is estimated to be vacant at all times, it can be rationalized by assuming that CO₂ dissociation occurs only on a se-

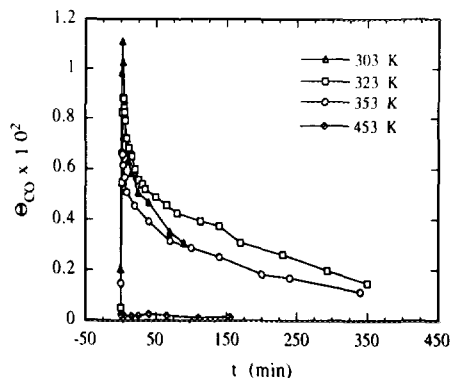


FIG. 13. Effect of temperature on the time-dependent coverage of Cu by CO during CO₂ exposure (150 Torr) of reduced Cu/SiO₂ at temperatures between 303 and 453 K.

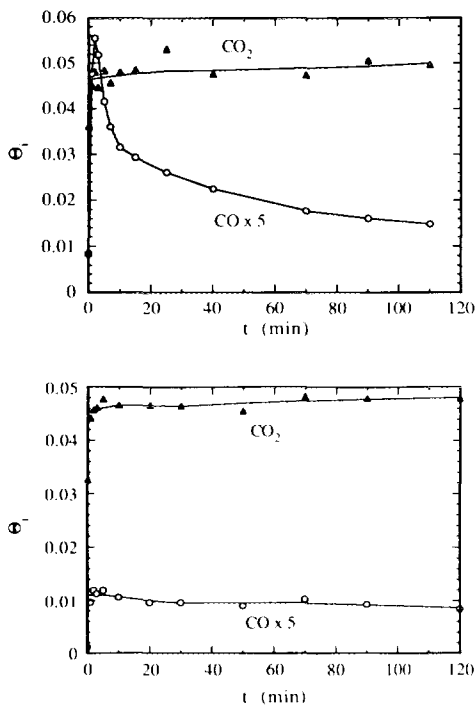


FIG. 14. Time-dependent coverages of Cu by CO and CO₂ during exposure of the catalyst to CO₂ at 303 K: (top) exposure of Cu/SiO₂ pre-reduced at 513 K in 1 atm H₂ for 20.5 h to $P_{\text{CO}_2} = 134$ Torr; (bottom) exposure of Cu/SiO₂ pre-reduced at 513 K in 1 atm H₂ for 18 h and then partially oxidized at 333 K in 76 Torr N₂O for 1.5 h to $P_{\text{CO}_2} = 162$ Torr.

lected portion of the Cu surface. Under such circumstances, the local concentrations of CO_s and O_s could become large enough to inhibit the dissociation of CO_{2,s}. Supporting the notion that dissociation occurs on a limited fraction of the Cu_s sites is the observation that the CO band is at 2118 cm⁻¹ even though the coverage by adsorbed CO based on total Cu_s sites is approximately 0.01. If CO_s and O_s were uniformly distributed, the adsorbed O_s would not be expected to perturb the position of the CO band. Moreover, competitive adsorption of CO and CO₂ could not occur unless the local surface concentrations were moderately high.

Additional experiments were performed to support the proposed mechanism for CO₂ dissociation. Figure 14 shows that preoxida-

tion of the catalyst at 363 K in N₂O inhibits the accumulation of CO_s, but not CO_{2,s}. On the other hand, Fig. 15 demonstrates that the addition of H₂ to the flow of CO₂ significantly enhances the formation of CO_s. It is noted as well that when the flow of H₂ is terminated, the surface concentration reverts to the level observed before the addition of H₂. Taken together, the results in Figs. 14 and 15 indicate that CO_{2,s} dissociation is inhibited by the accumulation of O_s on the catalyst surface. Besides facilitating further CO_{2,s} dissociation by removing O_s, H₂ may also favor dissociation by formation of a formate intermediate, as has recently been suggested by a BOC-MP analysis of the energetics of CO₂ hydrogenation on Cu (45).

CONCLUSIONS

At room temperature, CO₂ weakly adsorbs on Cu/SiO₂. Infrared evidence indicates that 24% of the adsorbed CO₂ is associated with the Cu and the balance with the silica support. CO₂ adsorbed on both Cu and SiO₂ is characterized by a band at 2340 cm⁻¹.

Room-temperature dissociation of adsorbed CO₂ produces CO_s and O_s. This process is retarded by preoxidation of the catalyst but proceeds more readily if H₂ is added to the gas phase. The CO formed by CO₂

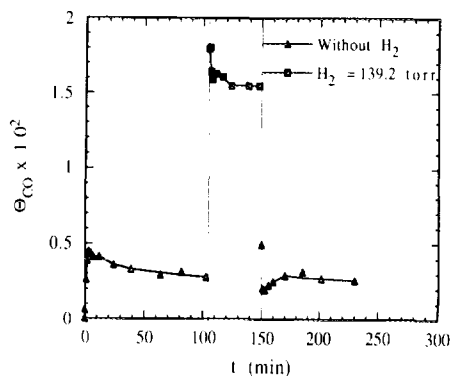


FIG. 15. Time-dependent coverage of Cu by CO and CO₂ during exposure of Cu/SiO₂ to $P_{\text{CO}_2} = 59$ Torr at 303 K. After 105 min, 139.2 Torr H₂ is cofed with CO₂. The H₂ is removed after 150 min.

dissociation exhibits an infrared band at 2118 cm^{-1} , characteristic of CO bonded to Cu^+ sites. From these observations, it is concluded that the CO_x and O_x produced upon dissociation of CO_2 remain in close proximity, the O_x being responsible for partial oxidation of the Cu.

The integrated absorption coefficient and the heat of adsorption have been determined for both CO and CO_2 . For CO the integrated absorption coefficient is $3.2 \times 10^{-17}\text{ cm}^{-1} \cdot \text{cm}^2/\text{molecule}$ and the heat of adsorption is 8.4 kcal/mol. For CO_2 adsorption the integrated absorption coefficient is $2.2 \times 10^{-17}\text{ cm}^{-1} \cdot \text{cm}^2/\text{molecule}$ and the heat of adsorption is 6.9 kcal/mol.

ACKNOWLEDGMENT

This work was supported by the Director, Office of Basic Energy Sciences, Chemical Sciences Division of the U.S. Department of Energy under Contract DE-AC03-76SF00098.

REFERENCES

- Chinchen, G. C., Spencer, M. S., Waugh, K. C., and Whan, D. A., *J. Chem. Soc. Faraday Trans. 1* **83** (Faraday Symposium 21), 2193 (1987).
- Sheffer, G. R., and King, T. S., *J. Catal.* **116**, 488 (1989).
- Pritchard, J., Catterick, T., and Gupta, G. K., *Surf. Sci.* **53**, 1 (1975).
- Woodruff, D. P., Hayden, B. E., Prince, K., and Bradshaw, A. M., *Surf. Sci.* **123**, 397 (1982).
- Truong, C. M., Rodriguez, J. A., and Goodman, D. W., *Surf. Sci. Lett.* **271**, L385 (1992).
- Horn, K., Hussain, M., and Pritchard, J., *Surf. Sci.* **63**, 244 (1977).
- Pritchard, J., *Surf. Sci.* **79**, 231 (1979).
- de Jong, K. P., Geus, J. W., and Joziassse, J., *Appl. Surf. Sci.* **6**, 273 (1980).
- Roberts, D. L., and Griffin, G. L., *J. Catal.* **110**, 117 (1988).
- Kohler, M. A., Cant, N. W., Wainwright, M. S., and Trimm, D. L., *J. Catal.* **117**, 188 (1989).
- Millar, G. J., Rochester, C. H., and Waugh, K. C., *J. Chem. Soc. Faraday Trans.* **87**(9), 1467 (1991).
- Papp, H., *Surf. Sci.* **63**, 182 (1977).
- Andersson, S., *Surf. Sci.* **89**, 477 (1979).
- Sexton, B. A., *Chem. Phys. Lett.* **63**(3), 451 (1979).
- Wendelken, J. F., and Ulehla, M. V. K., *J. Vac. Sci. Technol.* **16**(2), 441 (1979).
- Yu, K. Y., Spicer, W. E., Lindau, I., Pianetta, P., and Lin, S. F., *Surf. Sci.* **57**, 157 (1976).
- Allyn, C. L., Gustafsson, T., and Plummer, E. W., *Solid State Commun.* **24**, 531 (1977).
- Cox, D. F., and Schulz, K. H., *Surf. Sci.* **249**, 138 (1991).
- Harendt, C., Goschnick, J., and Hirschwald, W., *Surf. Sci.* **152/153**, 453 (1985).
- Tracy, J. C., *J. Chem. Phys.* **56**, 2748 (1972).
- Kessler, J., and Thieme, F., *Surf. Sci.* **67**, 405 (1977).
- Pritchard, J., *J. Chem. Soc. Faraday Trans.* **59**, 437 (1963).
- Netzer, F. P., Wille, R. A., and Matthew, J. A. D., *Solid State Commun.* **21**, 97 (1977).
- Spitzer, A., and Luth, H., *Surf. Sci.* **102**, 29 (1981).
- Hermann, K., Bagus, P. S., and Constance, J. N., *Phys. Rev. B* **35**(18), 9467 (1987).
- Bagus, P. S., Bauschlicher, C. W., and Nelin, C. J., *J. Vac. Sci. Technol. A* **2**(2), 905 (1984).
- Chesters, M. A., Pritchard, J., and Sims, M. L., in "Adsorption-Desorption Phenomena" (F. Ricca, Ed.), Academic Press, London, 1972.
- London, J. W., and Bell, A. T., *J. Catal.* **31**, 96 (1973).
- Wachs, I. E., and Madix, R. J., *J. Catal.* **53**, 208 (1978).
- Nakamura, J., Rodriguez, J. A., and Campbell, C. T., submitted for publication.
- Schneider, T., and Hirschwald, W., *Catal. Lett.* **14**, 197 (1992).
- Rasmussen, P. B., Taylor, P. A., and Chorkendorff, I., *Surf. Sci.* **269/270**, 352 (1992).
- Norton, P. R., and Tapping, R. L., *Chem. Phys. Lett.* **38**(2), 207 (1976).
- Copperthwaite, R. G., Davies, P. R., Morris, M. A., Roberts, M. W., and Ryder, R. A., *Catal. Lett.* **1**, 11 (1988).
- Hadden, R. A., Vandervell, H. D., Waugh, K. C., and Webb, G., *Catal. Lett.* **1**, 27 (1988).
- Millar, G. J., Rochester, C. H., Howe, C., and Waugh, K. C., *Mol. Phys.* **76**(4), 833 (1991).
- Kohler, M. A., Lee, J. C., Trimm, D. L., Cant, N. W., and Wainwright, M. S., *Appl. Catal.* **31**, 309 (1987).
- Parris, G. E., and Klier, K., *J. Catal.* **97**, 374 (1986).
- Hicks, R. F., Kellner, C. S., Savatsky, B. J., Hecker, W. C., and Bell, A. T., *J. Catal.* **71**, 216 (1981).
- Evans, J. W., Wainwright, M. S., Bridgewater, A. J., and Young, D. J., *Appl. Catal.* **7**, 75 (1983).
- Kohler, M. A., Curry-Hyde, H. E., Hughes, A. E., Sexton, B. A., and Cant, N. W., *J. Catal.* **108**, 323 (1987).
- Hicks, R. F., and Bell, A. T., *J. Catal.* **90**, 205 (1984).
- Winslow, P., and Bell, A. T., *J. Catal.* **86**, 158 (1984).
- Force, E. L., and Bell, A. T., *J. Catal.* **38**, 440 (1975).
- Shustorovich, E., and Bell, A. T., *Surf. Sci.* **253**, 386 (1991).